TauFlowNet: Uncovering Propagation Mechanism of Tau Aggregates by Neural Transport Equation

Tingting Dan[1], Minjeong Kim[2], Won Hwa Kim[3], and Guorong Wu[1,4(✉)]

[1] Department of Psychiatry, University of North Carolina at Chapel Hill, Chapel Hill, NC 27599, USA
guorong_wu@med.unc.edu

[2] Department of Computer Science, University of North Carolina at Greensboro, Greensboro, NC 27402, USA

[3] Computer Science and Engineering/Graduate School of AI, POSTECH, Pohang 37673, South Korea

[4] Department of Computer Science, University of North Carolina at Chapel Hill, Chapel Hill, NC 27599, USA

Abstract. Alzheimer's disease (AD) is characterized by the propagation of tau aggregates throughout the brain in a prion-like manner. Tremendous efforts have been made to analyze the spatiotemporal propagation patterns of widespread tau aggregates. However, current works focus on the change of focal patterns in lieu of a system-level understanding of the tau propagation mechanism that can explain and forecast the cascade of tau accumulation. To fill this gap, we conceptualize that the intercellular spreading of tau pathology forms a dynamic system where brain region is ubiquitously wired with other nodes while interacting with the build-up of pathological burdens. In this context, we formulate the biological process of tau spreading in a principled potential energy transport model (constrained by brain network topology), which allows us to develop an explainable neural network for uncovering the spatiotemporal dynamics of tau propagation from the longitudinal tau-PET images. We first translate the transport equation into a backbone of graph neural network (GNN), where the spreading flows are essentially driven by the potential energy of tau accumulation at each node. Further, we introduce the total variation (TV) into the graph transport model to prevent the flow vanishing caused by the $\updownarrow_2$-norm regularization, where the nature of system's Euler-Lagrange equations is to maximize the spreading flow while minimizing the overall potential energy. On top of this min-max optimization scenario, we design a generative adversarial network (GAN) to depict the TV-based spreading flow of tau aggregates, coined *TauFlowNet*. We evaluate *TauFlowNet* on ADNI dataset in terms of the prediction accuracy of future tau accumulation and explore the propagation mechanism of tau aggregates as the disease progresses. Compared to current methods, our physics-informed method yields more accurate and interpretable results, demonstrating great potential in discovering novel neurobiological mechanisms.

Keywords: Deep neural network · Complex system · Variational analysis · Total variation · Alzheimer's disease

H. Greenspan et al. (Eds.): MICCAI 2023, LNCS 14222, pp. 77–86, 2023.
https://doi.org/10.1007/978-3-031-43898-1_8

1 Introduction

Tau accumulation in the form of neurofibrillary tangles in the brain is an important pathology hallmark in Alzheimer's disease (AD) [1, 2]. With the rapid development of imaging technology, tau positron emission tomography (PET) allows us to measure the local concentration level of tau pathology *in-vivo*, which is proven to be a valuable tool for the differential diagnosis of dementia in routine clinical practice. As the converging consensus that the disease progression is closely associated with the spreading of tau aggregates [3], it is vital to characterize the spatiotemporal patterns of tau propagation from the longitudinal tau-PET scans.

The human brain is a complex system that is biologically wired by white matter fibers [4]. Such an optimized information-exchanging system supports transient self-organized functional fluctuations. Unfortunately, the concept of fast transport also applies to toxic tau proteins that hijack the network to spread rapidly throughout the brain. As shown in Fig. 1(a), the stereotypical spreading of the tau pathology facilitates the increase of whole-brain tau SUVR (standard uptake value ratio) as the stage of the disease progresses from mild to severe. In this context, many graph diffusion models have been proposed to model the temporal patterns of tau propagation. For example, the network diffusion model [5, 6] has been used to predict the future accumulation of pathological burdens where the spreading pathways are constrained by the network topology.

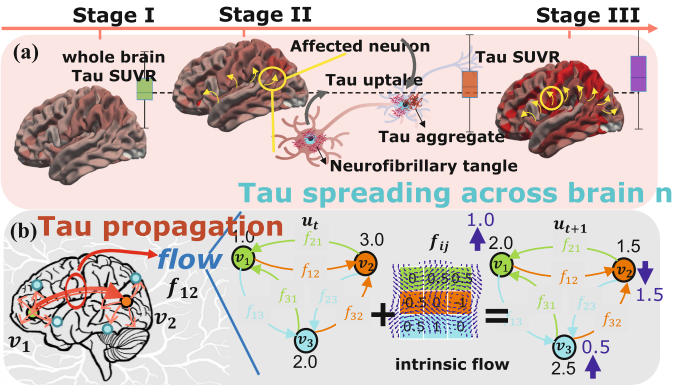

Fig. 1. **(a).** Tau spreading across the brain network facilitates the build-up of tau aggregates in the disease progression. **(b).** The illustration of the computational challenge for estimating the spreading flow of tau aggregates based on the change of focal patterns.

However, current computational models usually assume the system dynamics is a linear process [7–9], where such gross simplification might be responsible for the inconsistent findings on tau propagation. For instance, the eigenvectors of graph Laplacian matrix (corresponding to the adjacency matrix of the underlying brain network) have been widely used as the basis functions to fit the longitudinal changes of pathological burdens on each brain region. Supposing that future changes follow the same dynamics, we can forecast the tau accumulations via extrapolation in the temporal domain. It

is clear that these methods only model the focal change at each node, with no power to explain the tau propagation mechanism behind the longitudinal change, such as the questions "Which regions are actively disseminating tau aggregates?", "Does no change of tau SUVR indicate not being affected or just passing on the tau aggregates?".

To answer these fundamental questions, we put our spotlight on the spreading flows of tau aggregates. As shown in Fig. 1(b), it is computationally challenging to find the directed region-to-region flows that can predict the tau accumulations over time. We cast it into a well-posed problem by assuming the local development of tau pathology and the spreading of tau aggregates form a dynamic energy transport system [10]. In the analogy of gravity that makes water flow downward, the cascade of tau build-up generates a potential energy field (PEF) that drives the spreading of tau aggregates to propagate from high to low tau SUVR regions. As we constrain the tau spreading flows on top of the network topology, we translate the tau-specific transport equation into an equivalent graph neural network (GNN) [11], where the layer-by-layer manner allows us to effectively characterize the tau spreading flows from a large amount of longitudinal tau-PET scans. Since the deep model of GNN often yields over-smoothed PEF, we further tailor a new transport equation by introducing the total variation (TV) on the gradient of PEF, which prompts a new deep model (coined *TauFlowNet*) free of the vanishing flow issue. Specifically, we trace the root cause of the over-smoothing issue in GNN up to the $\updownarrow_2$-norm Lagrangian mechanics of graph diffusion process that essentially encourages minimizing the squared energy changes. Thus, one possible solution is to replace the $\updownarrow_2$-based regularization term with the TV constraint on the gradient of PEF. After that, the Euler-Lagrange (E-L) equation of the new Lagrangian mechanics describes new dynamics of tau propagation steered by a collection of max flows that minimize the absolute value of overall potential energies in the system. In this regard, we present a generative adversarial network (GAN) to find the max flows (in the discriminator model) that (i) follow the physics principle of transport equation (in the generator model) and (ii) accurately predict the future tau accumulation (as part of the loss function). Therefore, our *TauFlowNet* is an explainable deep model to the extent that the physics principle provides the system-level underpinning of tau spreading flows and the application value (such as prediction accuracy) is guaranteed by the mathematics insight and the power of deep learning.

We have applied our *TauFlowNet* on the longitudinal neuroimaging data in ADNI dataset. We compare the prediction accuracy of future tau accumulation with the counterpart methods and explore the propagation mechanism of tau aggregates as the disease progresses, where our physics-informed deep model yields more accurate and interpretable results. The promising results demonstrate great potential in discovering novel neurobiological mechanisms of AD through the lens of machine learning.

2 Methods

In the following, we first elucidate the relationship between GNN, E-L equation, and Lagrangian mechanics, which sets the stage for the method formulation and deep model design of our *TauFlowNet* in Sect. 2.1. Then, we propose the TV-based graph regularization for GAN-based deep learning in Sect. 2.2, which allows us to characterize the spreading flow of tau aggregates from longitudinal tau-PET scans.

Suppose the brain network is represented by a graph $\mathcal{G} = (V, W)$ with N nodes (brain regions) $V = \{v_i | i = 1, \ldots, N\}$ and the adjacency matrix $W = \left[w_{ij}\right]_{i,j=1}^{N} \in \mathcal{R}^{N \times N}$ describing connectivity strength between any two nodes. For each node v_i, we have a graph embedding vector $x_i \in \mathcal{R}^m$. The gradient $(\nabla_{\mathcal{G}} x)_{ij} = w_{ij}(x_i - x_j)$ indicates the feature difference between v_i and v_j weighed by the connectivity strength w_{ij}. Thus, the graph diffusion process [12] can be formulated as $\frac{\partial x(t)}{\partial t} = \text{div}(\nabla_{\mathcal{G}} x(t))$, where the evolution of embedding vectors $x = [x_i]_{i=1}^{N}$ is due to network flux measured by the *divergence*. Several decades ago, the diffusion process $\frac{\partial x(t)}{\partial t} = \text{div}(\nabla x(t))$ has been widely studied in image processing [13], which is the E-L equation of the functional $\min_x \int_\Omega |\nabla x|^2 dx$. By replacing the 1D gradient operator $(\nabla x)_{ij} = x_i - x_j$ defined in the Euclidean space Ω with the graph gradient $(\nabla_{\mathcal{G}} x)_{ij}$, it is straightforward to find that the governing equation in graph diffusion process $\frac{\partial x(t)}{\partial t} = \text{div}(\nabla_{\mathcal{G}} x(t))$ is the E-L equation of functional $\min_x \int_{\mathcal{G}} \left|\nabla_{\mathcal{G}} x\right|^2 dx$ on top of the graph topology.

The GNN depth is blamed for over-smoothing [14–16] in graph representation learning. We attribute this to the isotropic smoothing mechanism formulated in the $\updownarrow_2$-norm. Connecting GNN to calculus of variations provides a principled way to design new models with guaranteed mathematics and explainability.

2.1 Problem Formulation for Discovering Spreading Flow of Tau Propagation

Neuroscience Assumption. Our brain's efficient information exchange facilitates the rapid spread of toxic tau proteins throughout the brain. To understand this spread, it's essential to measure the intrinsic flow information (such as flux and bandwidth) of tau aggregates in the complex brain network.

Problem Formulation from the Perspective of Machine Learning. The overarching goal is to estimate the time-dependent flow field $f(t) = \left[f_{ij}(t)\right]_{i,j=1}^{N}$ of tau spreading such that $x_i(t+1) = x_i(t) + \sum_{j=1}^{N} f_{ij}(t)$, where $f_{ij}(t)$ stands for the directed flow from the region v_i to v_j. As the toy example shown in Fig. 1(b), there are numerous possible solutions for F given the longitudinal change Δx. To cast this ill-posed problem into a well-defined formulation, we conceptualize that the tau propagation in each brain forms a unique dynamic transport system of the brain network, and the spreading flow is driven by a tau-specific potential energy field $u(t) = [u_i(t)]_{i=1}^{N}$, where $u_i(t)$ is output of a nonlinear process ϕ reacting to the tau accumulation x_i at the underlying region v_i, i.e., $u_i = \phi(x_i)$. The potential energy field drives the flow of tau aggregates in the brain, similar to the gravity field driving water flow. Thereby the spreading of tau is defined by the gradient of potential energy between connected regions:

$$f_{ij}(t) = -\left(\nabla_{\mathcal{G}} u(t)\right)_{ij} = -w_{ij}\left(u_i(t) - u_j(t)\right), \tag{1}$$

Thus, the fundamental insight of our model is that the spreading flow $f_{ij}(t)$ is formulated as an "energy transport" process of the tau potential energy field. Taking together, the output of our model is a mechanistic equation $M(\cdot)$ of the dynamic system that can predict the future flow based on the history flow sequences, *i.e.*, $\hat{f}_{ij}(t_T) = M\left(f_{ij}(t_1), \ldots, f_{ij}(t_{T-1})\right)$.

Transport Equation for Tau Propagation in the Brain. A general continuity transport equation [10] can be formulated in a partial differential equation (PDE) as:

$$\frac{dx}{dt} + div(q) = 0 \tag{2}$$

where q is the flux of the potential energy u (conserved quantity). The intuition of Eq. 2 is that the change of energy density (measured by regional tau SUVR x) leads to the energy transport throughout the brain (measured by the flux of PEF). As flux is often defined as the rate of flow, we further define the energy flow as $q_{ij} = \alpha \cdot f_{ij}$, where α is a learnable parameter characterizing the contribution of the tau flow f_{ij} to the potential energy flux q_{ij}. By plugging $u_t = \phi(x_t)$ and $q_{ij} = \alpha \cdot f_{ij}$ into Eq. 2, the energy transport process of tau spreading flow f can be described as:

$$\frac{\partial u}{\partial t} = -\phi\Big(\alpha^{-1} div(f)\Big). \tag{3}$$

Note, ϕ and α are trainable parameters that can be optimized through the supervised learning schema described below.

2.2 *TauFlowNet*: An Explainable Deep Model Principled with TV-Based Lagrangian Mechanics

To solve the flow field f in Eq. 3, the naïve deep model is a two-step approach (shown in the left red panel of Fig. 2).

(1) *Estimate the PEF u by fixing the flow f.* By letting $f = \nabla_{\mathcal{G}} u$ (in Eq. 1), the solution of u follows a reaction process $u = \phi(x)$ and a graph diffusion process $\frac{\partial u}{\partial t} = -\alpha^{-1} div\big(\nabla_{\mathcal{G}} u\big) = -\alpha^{-1}\Delta u$, where $\Delta = div(\nabla_{\mathcal{G}})$ is the graph Laplacian operator. The parameters of ϕ and α can be learned using a multi-layer perceptron (MLP) and a graph convolution layer (GCN), respectively. Thus, the input is the observed tau SUVR x_t and the loss function aims to minimize the prediction error from x_t to x_{t+1}.

(2) *Calculate spreading flow f.* Given u, it is straightforward to compute each flow $f_{ij}(t)$ by Eq. 1. In Sect. 2.1, we have pointed out that the GNN architecture is equivalent to the graph diffusion component in Eq. 3. Since the PDE of the graph diffusion process $\frac{\partial u}{\partial t} = -\Delta u$ is essentially the Euler-Lagrange (E-L) equation of the quadratic functional $\mathcal{J}(u) = \min_u \int \big(\nabla_{\mathcal{G}} u\big)^2 du$, the major issue is the "over-smoothness" in u that might result in vanishing flows (*i.e.*, $f \to 0$).

To address the over-smoothing issue, we propose to replace the quadratic Laplacian regularizer with total variation, i.e., $\mathcal{J}_{TV}(u) = \min_u \int \big|\nabla_{\mathcal{G}} u\big| du$, which has been successfully applied in image denoising [17] and reconstruction [18]. Since $|\cdot|$ in $\mathcal{J}_{TV}$ is not differentiable at 0, we introduce the latent flow variable f and reformulate the TV-based functional as $\mathcal{J}_{TV}(u, f) = \min_u \int (f \otimes \nabla_{\mathcal{G}} u) du$, where $\otimes$ is Hadamard operation between two matrices. Recall that the flow f_{ij} has directionality. Thus, the engineering trick of element-wise operation $f_{ij}\big(\nabla_{\mathcal{G}} u\big)_{ij}$ keeps the degree always non-negative as we take the absolute value, which allows us to avoid the undifferentiable challenge.

After that, we boil down the minimization of $\mathcal{J}_{TV}(u)$ into a dual min-max functional as $\mathcal{J}_{TV}(u,f) = \min_{u}\max_{f} \int \big(f \cdot \nabla_{\mathcal{G}} u\big) du$, where we maximize f such that $\mathcal{J}_{TV}(u,f)$ is close enough to $\mathcal{J}_{TV}(u)$. In this regard, the E-L equation from the Gâteaux variations leads to two coupled PDEs:

$$\begin{cases} \max\limits_{f} \frac{df}{dt} = \nabla_{\mathcal{G}} u \\ \min\limits_{u} \frac{du}{dt} = div(f) \end{cases} \tag{4}$$

The alternative solution for Eq. 4 is that we minimize PEF u through the Lagrangian mechanics defined in the transport equation $\frac{\partial u}{\partial t} = -\phi\big(\alpha^{-1} div(f)\big)$ where the system dynamics is predominated by the maximum flow field f. Since the accurate estimation of flow field $f(t)$ and PEF $u(t)$ is supposed to predict the future tau accumulation $x(t+1)$ by $x_i(t+1) = \phi^{-1}\Big(u_i(t) + \sum_{j=1}^{N} f_{ij}(t)\Big)$, we can further tailor the min-max optimization for Eq. 4 into a supervised learning scenario as the *TauNetFlow* described next.

TauFlowNet: A GAN Network Architecture of TV-Based Transport Equation. Here, we present an explainable deep model to uncover the spreading flow of tau aggregates f from the longitudinal tau-PET scans. Our deep model is trained to learn the system dynamics (in Eq. 4), which can predict future tau accumulations. The overall network architecture of *TauFlowNet* is shown in Fig. 2, which consists of a generator (left) and a discriminator module (right). The generator is essentially our initial GNN model of the transport equation that consists of a reaction process ϕ and a graph diffusion process. Specifically, the generator consists of (i) a MLP to project the input regional tau SUVR x_t into the potential energy filed u_t through a nonlinear reaction process $u_t = \phi(x_t)$ (green dashed box), (ii) a GCN layer to transport potential energy along the connectome pathways, resulting in the $u_{t+1} = GCN(u_t)$ (purple dashed box), and (iii) another MLP to generate $\hat{x}_{t+1}$ from u_{t+1} via $\hat{x}_{t+1} = \phi^{-1}(u_{t+1})$ (red dashed box). The discriminator module is designed to synthesize the future PEF u_{t+1} based on the current PEF u_t and current estimation of tau spreading flow f_{ij} (orange dash box), i.e., $\tilde{u}_{t+1} = u_t + \sum_{j=1}^{N} f_{ij}(t)$. Then, we train another GCN layer to generate the synthesized $\tilde{x}_{t+1}$ from $\tilde{u}_{t+1}$ via $\tilde{x}_{t+1} = GCN(\tilde{u}_{t+1})$ (blue dashed box).

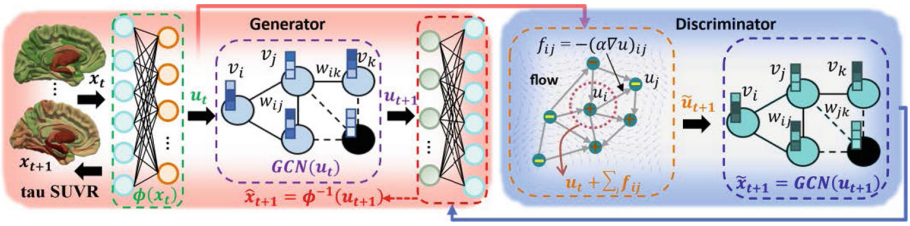

Fig. 2. The GAN architecture for min-max optimization in the *TauFlowNet*. (Color figure online)

The driving force of our *TauFlowNet* is to minimize (1) the MAE (mean absolute error) between the output of the generator $\hat{x}_{t+1}$ and the observed tau SUVR, and (2) the

distance between the synthesized tau SUVR $\tilde{x}_{t+1}$ (from the discriminator) and the output of generator $\hat{x}_{t+1}$ (from the transport equation). In the spirit of probabilistic GAN [19], we use one loss function $\mathcal{L}_D = D(x_{t+1}) + [m - D(G(x_t))]^+$ to train the discriminator (D) and the other one $\mathcal{L}_G = D(G(x_t))$ to train the generator (G), where m denotes the positive margin and the operator $[\cdot]^+ = \max(0, \cdot)$. Minimizing $\mathcal{L}_G$ is similar to maximizing the second term of $\mathcal{L}_D$ except the non-zero gradient when $D(G(x_t)) \geq m$.

3 Experiments

In this section, we evaluated the performance of the proposed *TauFlowNet* for uncovering the latent flow of tau spreading on the Alzheimer's Disease Neuroimaging Initiative (ADNI) dataset (https://adni.loni.usc.edu/). In total, 163 subjects with longitudinal tau-PET scans are used for training and testing the deep model. In addition, each subject has T1-weighted MRI and diffusion-weighted imaging (DWI) scan, from which we construct the structural connectome. Destrieux atlas [20] is used to parcellate each brain into 160 regions of interest (ROIs), which consist of 148 cortical regions (frontal lobe, insula lobe, temporal lobe, occipital lobe, parietal lobe, and limbic lobe) and 12 sub-cortical regions (left and right hippocampus, caudate, thalamus, amygdala, globus pallidum, and putamen). Following the clinical outcomes, we partition the subjects into the cognitive normal (CN), early-stage mild cognitive impairment (EMCI), late-stage MCI (LMCI), and AD groups. We compare our *TauFlowNet* with classic graph convolutional network (GCN) [21] and deep neural network (DNN) [22]. We use 5-fold cross-validation to evaluate the prediction performance and examine the spreading patterns of tau aggregates in different clinic groups.

3.1 Evaluate the Prediction Accuracy of Future Tau Accumulation

We first evaluate the prediction performance between the ground truth and the estimated SUVR values, where we use the mean absolute error (MAE) to quantify the prediction accuracy. The statistics of MAE by our *TauFlowNet*, GCN, and DNN are shown in the first column (with shade) of Table 1. To further validate the robustness of our model, we add uncorrelated additive Gaussian noises to the observed SUVR measurements. The prediction accuracies with respect to different noise levels are listed in the rest columns of Table 1. It is clear that our *TauFlowNet* consistently outperforms the other two deep models. The performance of GCN is worse than DNN within the same network depth, which might be due to the over-smoothing issue.

As part of the ablation study, we implement the two-step approach (the beginning of Sect. 2.2), where we train the model (MLP + GCN) shown in the left panel of Fig. 2 to obtain further tau accumulation. Since the deep model in this two-step approach is formalized from the PDE, we call this degraded version as *PDENet*. We display the result of in the last row of Table 1. Compared to *PDENet*, our *TauFlowNet* (in GAN architecture) takes advantage of TV constraint to avoid over-smoothing and integrates two steps (i.e., estimating PEF and uncovering spreading flows) into a unified neural network, thus significantly enhancing the prediction accuracy.

Table 1. The prediction performance (MAE) between observed and predicted tau.

Noise level	–	std = 0.02	std = 0.04	std = 0.08	std = 0.1
TauFlowNet	**0.049 ± 0.02**	**0.058 ± 0.03**	**0.066 ± 0.03**	**0.079 ± 0.04**	**0.081 ± 0.04**
GCN	0.124 ± 0.08	0.128 ± 0.08	0.130 ± 0.08	0.142 ± 0.08	0.161 ± 0.10
DNN	0.070 ± 0.03	0.072 ± 0.04	0.080 ± 0.04	0.104 ± 0.06	0.112 ± 0.06
PDENet	0.110 ± 0.05	0.120 ± 0.05	0.128 ± 0.05	0.134 ± 0.05	0.155 ± 0.06

3.2 Examine Spatiotemporal Patterns of the Spreading Flow of Tau Aggregates

We examine the pattern of spreading flows on an individual basis (Fig. 3a) and cross populations (Fig. 3b). *First*, we visualize the top flows (ranked in terms of flow volume) uncovered in a CN subject. It is apparent that subcortex-cortex flows are the predominant patterns, where most of the tau aggregates spread from subcortical regions (globus pallidus, hippocampus, and putamen) to the temporal lobe, limbic lobe, parietal lobe, and insula lobe. Note, we find inferior temporal gyrus (t_6) and entorhinal cortex (t_8) are actively involved in the subcortex-cortex flows, which are the footprints of early stage tau propagation frequently reported in many pathology studies [23]. *Second*, we show the top-ranked population-wise average tau spreading flows for CN, EMCI, LMCI, and AD groups in Fig. 3b. As the disease progresses, the subcortex-cortex flows gradually switch to cortex-cortex flows. After tau aggregates leave the temporal lobe, the tau propagation becomes widespread throughout the entire cortical region.

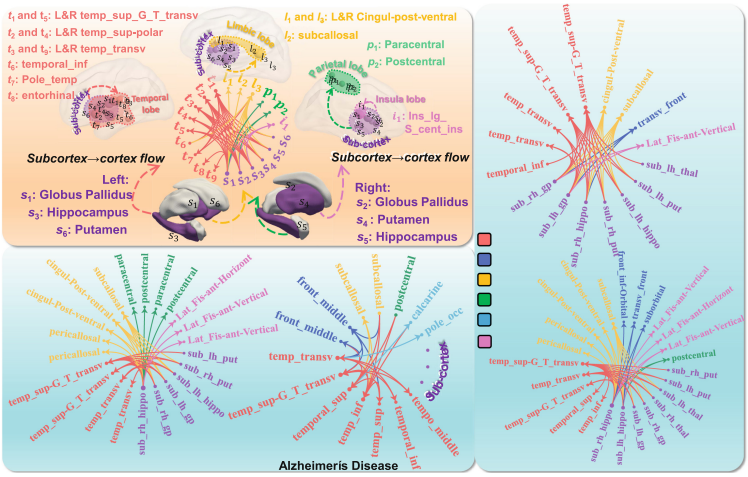

Fig. 3. Visualization of tau spreading flows in an individual cognitive normal subject (a) and the population-wise average spreading flows for CN, early/late-MCI, and AD groups.

4 Conclusion

In this paper, we propose a physics-informed deep neural network (*TauFlowNet*) by combining the power of dynamic systems (with well-studied mechanisms) and machine learning (fine-tuning the best model) to discover the novel propagation mechanism of tau spreading flow from the longitudinal tau-PET scans. We have evaluated our *TauFlowNet* on ADNI dataset in forecasting tau accumulation and elucidating the spatiotemporal patterns of tau propagation in the different stages of cognitive decline. Our physics-informed deep model outperforms existing state-of-the-art methods in terms of prediction accuracy and model explainability. Since the region-to-region spreading flow provides rich information for understanding the tau propagation mechanism, our learning-based method has great applicability in current AD studies.

Acknowledgment. This work was supported by Foundation of Hope, NIH R01AG068399, NIH R03AG073927. Won Hwa Kim was partially supported by IITP-2019-0-01906 (AI Graduate Program at POSTECH) funded by the Korean government (MSIT).

References

1. Jack, C.R., et al.: NIA-AA research framework: toward a biological definition of Alzheimer's disease. Alzheimers Dement. **14**(4), 535–562 (2018)
2. Al Mamun, A., et al.: Toxic tau: structural origins of tau aggregation in Alzheimer's disease. Neural Regen. Res. **15**(8), 1417 (2020)
3. Goedert, M., Eisenberg, D.S., Crowther, R.A.: Propagation of Tau aggregates and neurodegeneration. Annu. Rev. Neurosci. **40**(1), 189–210 (2017)
4. Bassett, D.S., Sporns, O.: Network neuroscience. Nat. Neurosci. **20**(3), 353–364 (2017)
5. Raj, A., Kuceyeski, A., Weiner, M.: A network diffusion model of disease progression in dementia. Neuron **73**(6), 1204–1215 (2012)
6. Zhang, J., et al.: A network-guided reaction-diffusion model of AT [N] biomarkers in Alzheimer's disease. In: 2020 IEEE 20th International Conference on Bioinformatics and Bioengineering (BIBE). IEEE (2020)
7. Raj, A., et al.: Network diffusion model of progression predicts longitudinal patterns of atrophy and metabolism in Alzheimer's disease. Cell Rep. **10**(3), 359–369 (2015)
8. Raj, A., Powell, F.: Network model of pathology spread recapitulates neurodegeneration and selective vulnerability in Huntington's disease. Neuroimage **235**, 118008 (2021)
9. Vogel, J.W., et al.: Spread of pathological tau proteins through communicating neurons in human Alzheimer's disease. Nat. Commun. **11**(1), 2612 (2020)
10. Arnold, V.I.: Mathematical Methods of Classical Mechanics. Graduate Texts in Mathematics Mathematics. Springer, New York (1978). https://doi.org/10.1007/978-1-4757-1693-1
11. Zhou, J., et al.: Graph neural networks: a review of methods and applications. AI Open **1**, 57–81 (2020)
12. Chamberlain, B., et al.: Grand: graph neural diffusion. In: International Conference on Machine Learning. PMLR (2021)
13. Matallah, H., Maouni, M., Lakhal, H.: Image restoration by a fractional reaction-diffusion process. Int. J. Anal. Appl. **19**(5), 709–724 (2021)
14. Li, G., et al.: DeepGCNs: can GCNs go as deep as cnns? In: Proceedings of the IEEE/CVF International Conference on Computer Vision (2019)

15. Xu, K., et al.: Representation learning on graphs with jumping knowledge networks. In: International Conference on Machine Learning. PMLR (2018)
16. Chen, M., et al.: Simple and deep graph convolutional networks. In: International Conference on Machine Learning. PMLR (2020)
17. Rudin, L.I., Osher, S., Fatemi, E.: Nonlinear total variation based noise removal algorithms. Physica D **60**(1), 259–268 (1992)
18. Chan, T., et al.: Total variation image restoration: overview and recent developments. In: Paragios, N., Chen, Y., Faugeras, O. (eds.) Handbook of Mathematical Models in Computer Vision, pp. 17–31. Springer, Boston (2006). https://doi.org/10.1007/0-387-28831-7_2
19. Zhao, J., Mathieu, M., LeCun, Y.: Energy-based generative adversarial network. arXiv preprint arXiv:1609.03126 (2016)
20. Destrieux, C., et al.: Automatic parcellation of human cortical gyri and sulci using standard anatomical nomenclature. Neuroimage **53**(1), 1–15 (2010)
21. Zhang, H., et al.: Semi-supervised classification of graph convolutional networks with Laplacian rank constraints. Neural Process. Lett. 1–12 (2021)
22. Riedmiller, M., Lernen, A.: Multi layer perceptron. Machine Learning Lab Special Lecture, pp. 7-24. University of Freiburg (2014)
23. Lee, W.J., et al.: Regional Aβ-tau interactions promote onset and acceleration of Alzheimer's disease tau spreading. Neuron (2022)